HEAVY FLAVOR PRODUCTION AND DECAY*

J.H. KÜHN**

Institut für Theoretische Teilchenphysik, Universität Karlsruhe,
D-76128 Karlsruhe, Germany

(Received January 14, 1997)

Recent theoretical results on heavy flavor production and decay in the framework of perturbative QCD are reviewed. This includes calculations for top production at hadron colliders, inclusive charmonium production and the comparison between the singlet and octet mechanisms. Predictions for heavy flavor production in e^+e^- annihilation will be discussed in some detail, covering both the threshold and the high energy region. The first results in NLO for heavy flavor decays will also be reviewed.

PACS numbers: 12.38. Cy

1. Introduction

Heavy flavor production and decay have developed into benchmark reactions for perturbative QCD. The large energy scale inherent in most of these reactions allows for a separation between hard and soft momentum transfers. The former can be treated perturbatively, the nonperturbative matrix elements which encode the remaining information can either be determined experimentally, or integrated out by considering sufficiently inclusive information such that perturbation theory alone is adequate.

Significant progress has been achieved recently in a number of topics. The predictions for top production at hadron colliders have been scrutinized by several authors. In particular the role of soft gluon resummation has been emphasised and the α_s dependence explored (Section 2). Inclusive charmonium production at hadron and e^+e^- colliders has been studied theoretically and experimentally. A fairly complex picture seems to emerge, with different mechanisms playing a role in various reactions (Section 3). The inclusive cross section for heavy flavor production in e^+e^- annihilation

* Presented at the Cracow International Symposium on Radiative Corrections to the Standard Model, Cracow, Poland, August 1–5, 1996.

** Supported by BMBF contract 057KA92P.

has been studied in a variety of papers. Far above threshold an expansion in m^2/s is adequate and has been successfully applied to Z decays to bottom quarks, or to charm production just below the $b\bar{b}$ threshold. For a prediction above, but relatively close to threshold a different strategy has been employed, which is based on a combination of analytical and numerical methods. For an adequate treatment of top quark production in the threshold region its large decay rate and the interplay between gluon radiation from the production and the decay process must be taken into account. These topics will be reviewed in Section 4. The leading QCD correction to weak decays of heavy flavors have been evaluated quite some time ago. Results are available for the rate, the spectrum and for angular distributions. To match the level of precision claimed by the proponents of the Heavy Quark Effective Theory, next to leading order predictions are required from perturbation theory. First steps into this direction have been made and will be reviewed in Section 5.

2. Top production in hadronic collisions

The theoretical framework and the (semi-) analytical results for the top production cross section in NLO have been developed nearly a decade ago [1, 2]. The predictions for $\sqrt{s} = 1.8$ GeV and $m_t = 180$ GeV from various authors are listed in Table I.

TABLE I

History of predictions for the production cross section for $\sqrt{s} = 1.8$ TeV and $m_t = 180$ GeV.

	σ [pb]		
Altarelli *et al.* [2]	3.52 (DFLM)		
	4.10 (ELHQ)		
Laenen *et al.* [4]	3.5	$(\mu^2 = 4m^2)$	MRSD
	3.8	$(\mu^2 = m^2)$	MRSD
	4.05	$(\mu^2 = m^2/4)$	MRSD
Resummation			
Laenen *et al.* [4]	3.86	vary μ_0	
	4.21	vary μ_0	
	4.78	vary μ_0	
Berends *et al.* [3]	4.8 central value		
Berger *et al.* [5]	4.8 "principal value res."		
Catani *et al.* [6]	$4.05^{+0.62}_{-0.52}$		

For $m_t = 175$ GeV the cross section increases by about 0.7 pb. The uncertainty in the factorization and renormalisation scale leads to an uncertainty of roughly 10%. Recently the issue of soft gluon resummation has been raised. The original arguments [4, 5] leading to a large positive shift of roughly 10% have been refuted in [6]. No consensus has yet been reached on the magnitude of these effects. Increasing α_s from the nominal value of around 0.11, which has been frequently used in these calculations, to 0.120 leads to an increase by about 5%. Within the combined uncertainties theory and experiment are in very good agreement (Fig. 1).

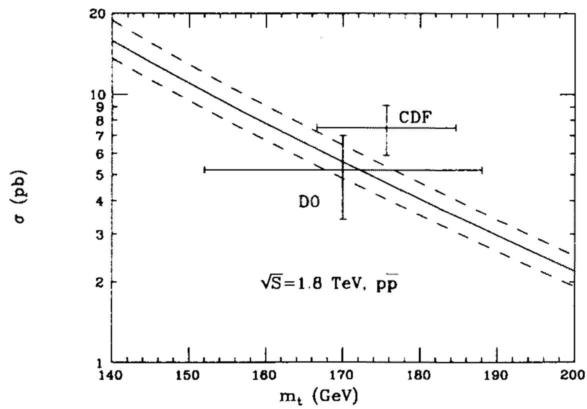

Fig. 1. Top cross section at the Tevatron at $\sqrt{S} = 2$ TeV (from [7]).

All these calculations are based on a perturbative treatment of the threshold region. In principle one should, however, incorporate the leading terms of order $\pi\alpha_s/\beta$. The resulting modifications are small for $t\bar{t}$ in a color octet which is the dominant configuration at the TEVATRON (see Section 2.2.2 in [8]).

3. Inclusive charmonium production

High energy hadron-hadron and e^-p colliders are charmonium factories. A variety of production mechanisms have been discussed in the literature. Contributing with different relative strengths in the various reactions they can be disentangled only through a systematic study of different processes. In particular the question of color singlet versus octet production has stimulated a number of detailed investigations.

Inelastic J/ψ production in photon-photon reactions provides a relatively clean testing ground. The dominant subprocess at the parton level

$$\gamma + g \to J/\psi + g \tag{1}$$

can produce directly a $(c\bar{c})$ color singlet state. Incorporating also the one loop perturbative corrections [9], satisfactory agreement between theory and experiment is observed for the J/ψ energy distributions and the total production cross section as well (Fig. 2).

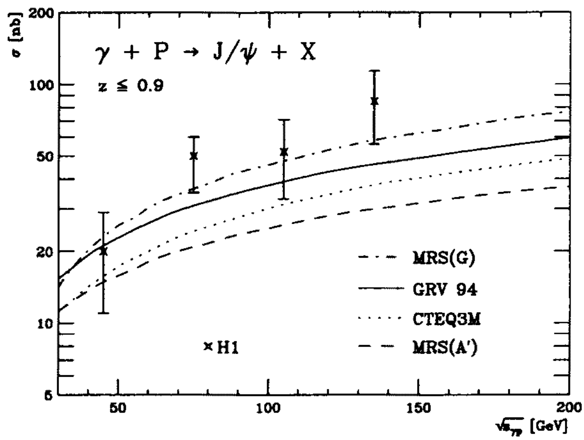

Fig. 2. Comparison between theoretical prediction for the energy dependence of the inelastic cross section ($z \leq 0.9$) for J/ψ photoproduction (J. Steegborn, private communication, based on [9]) and recent data from the H1 Collaboration.

This success of the color singlet model (CSM) (where quarkonium (color singlet!) states are required to be produced through a purely perturbative mechanism) is in marked contrast with its failure in purely hadronic collisions. The dominant subprocesses in the CSM are based on the conversion of a virtual gluon into J/ψ or χ_J plus two or one gluon respectively. The combination of additional powers of α_s with the small phase space gives rise to sizable suppression factors. This perturbative treatment of soft gluon radiation may be inadequate and an alternative approach has been advocated in [10]. The cross section for charmonium production is decomposed into a sum of terms consisting of the cross section for $(c\bar{c})$ states in a specific angular momentum and color state times the nonperturbative matrix element of an operator characterizing the conversion probability into J/ψ:

$$\sigma(p\bar{p} \to J/\psi + x) = \sum_n \sigma(p\bar{p} \to c\bar{c}(n)) \times \langle \mathcal{O}_n^{J/\psi} \rangle. \tag{2}$$

These matrix elements are effectively free parameters to be determined in different experiments. This approach is closely related in its spirit to the color evaporation model formulated a long time ago; it provides, however, a more firm theoretical formulation. Adjusting the parameters appropriately, a satisfactory description of the data is obtained.

The clean initial state configuration typical for e^+e^- annihilation is ideal to investigate the relative importance of different production mechanisms. Two distinctly different situations have been considered: high energy reactions like Z decays with large event rates available at LEP and alternatively the 10 GeV region that can be explored at present at CESR or in the near future at the B-meson factories. Three mechanisms have been identified at which contribute in the high energy region with comparable rates. The reaction [11]

$$Z \to J/\psi c\bar{c} + X \tag{3}$$

requires the production of two $c\bar{c}$ pairs with a rate proportional to $\alpha_s^2|R(0)|^2$. The second mechanism [12] is the splitting of a virtual gluon in a color octet $c\bar{c}$:

$$Z \to q\bar{q}(c\bar{c})_8 \tag{4}$$

with the subsequent nonperturbative conversion of $(c\bar{c})_8$ into J/ψ. The rate for this mechanism is proportional to $\alpha_s^2\langle \mathcal{O}^8\rangle$ where the second factor characterizes the nonperturbative matrix element. The third, color singlet, contribution [13]

$$Z \to q\bar{q}J/\psi gg \tag{5}$$

is strongly suppressed by the factor $\alpha_s^4|R(0)|^2$ and, furthermore, by the small phase space. The branching ratios of the three reactions are given by $0.8 \cdot 10^{-4}$, $1.9 \cdot 10^{-4}$, $0.2 \cdot 10^{-4}$, respectively. The total inclusive rate is reasonably consistent with the observations by the OPAL collaboration [14] of $(1.9 \pm 0.7 \pm 0.5 \pm 0.5) \cdot 10^{-4}$. However, a statement about the dominance of any of these processes seems premature. The analysis of J/ψ energy and momentum distributions, however, could help to settle this issue.

Also B meson factories and CESR give rise to a large sample of events with prompt J/ψ production. Two mechanisms have been proposed which might well describe complementary kinematical regions. The leading process in the CSM

$$e^+e^- \to J/\psi + gg \tag{6}$$

is proportional to $\alpha_s^2|R(0)|^2$. It leads to a three body final state and hence to a continuous energy distribution (Fig. 3).

Predictions for the rate, the angular and the momentum distribution and the polarization can be found in [15]. The alternative approach [16] is based on "color octet production", $e^+e^- \to (c\bar{c})_8 + g$. The rate is of order α_s and multiplied by a nonperturbative matrix element. The J/ψ energy

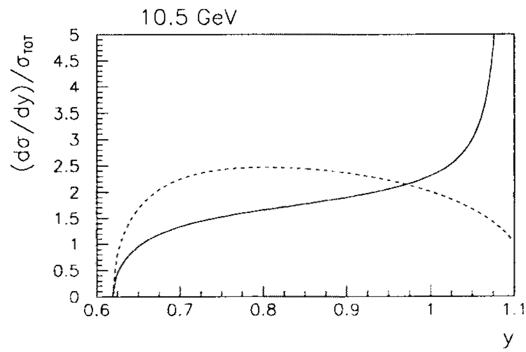

Fig. 3. Energy distribution for inclusive J/ψ production in e^+e^- annihilation at 10.5 GeV. Solid curve: $\alpha_s(M_{gg}^2)$, dashed curve $\alpha_s(M_\psi^2)$.

is essentially fixed at $E_{\text{max}} = (s + m_\psi^2)/(2\sqrt{s})$. The angular distribution is proportional to $(1 + \cos^2\theta)$. These features are identical to the predictions of the "color evaporation model" [17] formulated a long time ago. An excess of J/ψ at this special kinematical point with the predicted angular distribution would be a strong indication for this "octet mechanism". The angular distribution of the J/ψ in the CSM is of the form $1 + \alpha(y)\cos^2\theta$ where $\alpha(y)$ depends on $y \equiv E_\psi/E_{\text{Beam}}$ and approaches roughly -0.8 at the endpoint (Fig. 4). This difference will be crucial in disentangling the two mechanisms.

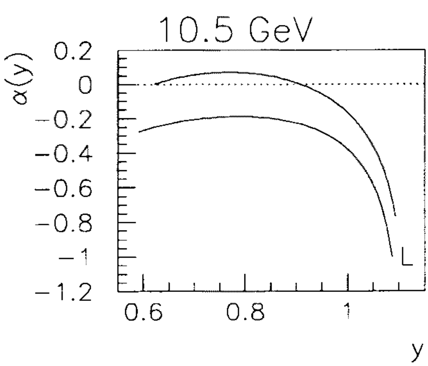

Fig. 4. Coefficient $\alpha(y)$ characterizing the angular distribution of J/ψ's (L: longitudinally polarized J/ψ's only).

4. Heavy flavor production in e^+e^- annihilation

4.1. $Z \to b\bar{b}$

Experimental studies of various partial and of the total Z decay rate have been performed recently with a new level of sophistication. The relative error in Γ_b has been lowered to about $0.5 \cdot 10^{-2}$ corresponding to $\delta\Gamma_b \approx 2.5$ MeV, the uncertainty in the total decay rate which is also influenced by Γ_b amounts to about 3 MeV. In comparison with Γ_d or Γ_u two important differences have to be taken into account for Γ_b. The first, relatively straightforward aspect is related to the bottom mass. In Born approximation the correction from the phase space suppression of the axial part of the rate is predicted to be $-6m_b^2/M_Z^2$ corresponding to -4 MeV. In [18] it has been demonstrated that this number is drastically modified by QCD corrections. The bulk of these, the large logarithms, can be absorbed by reexpressing the result in terms of the running mass thus reducing the correction to -1.6 MeV. (For a detailed discussion and further references see [19].) The second contribution to the $Z \to b\bar{b}$ decay has its origin in the double triangle diagrams with two gluon intermediate states. It is present for the axial rate only. The contribution of order α_s^2 was calculated quite some time ago for arbitrary m_t^2/M_Z^2. Formally it is proportional to $\ln m_t^2/M_Z^2$ and thus seems to diverge in the limit of large $\ln m_t^2/M_Z^2$. However, additional logarithms of m_t^2/μ^2 are induced by the running of α_s which have to be controlled at the same time. The structure of leading logs was analysed in [20], the constant terms of α_s^3 in [21]. The combined effect of order α_s^2 and α_s^3 from these "singlet terms" amounts $\delta\Gamma_b = -1.8$ MeV. It is clear that the sum of mass and singlet terms must be taken into consideration in any precision analysis.

4.2. Intermediate energies

The Z decay rate is well described in the massless approximation plus terms of order m_b^2/M_Z^2. However, for a prediction at lower energies, an increasing series of terms in the m^2/s expansion is needed. The comparison between the complete calculation and a limited number of terms in the m^2/s expansion indicates that the first three terms are sufficient to describe the cross section from high energies down to $s \approx 8m^2$. With this motivation in mind the quartic terms of order α_s^2 have been calculated in [22]. In this way an adequate prediction between roughly 14 GeV and M_Z is available for $b\bar{b}$ production, and similarly for $c\bar{c}$ production from roughly 5 to 6 GeV up to the bottom quark threshold [23] (Fig. 5).

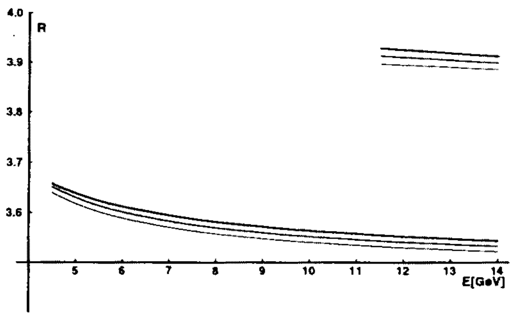

Fig. 5. The ratio $R(s)$ below and above the b quark production threshold at 10.5 GeV for $\alpha_s(M_Z) = 0.120$, 0.125 and 0.130. The contributions from light quarks (u, d, s, c) and the bottom quark are displayed separately.

In view of the large statistics available at CESR and at a future B-meson factory a detailed theoretical study has been performed in [24] which demonstrates the potential for this potentially most precise and clean determination of α_s.

4.3. The NLO calculation for arbitrary m^2 and s

A few GeV above charm, bottom, or top threshold measurements can in principle be performed at a τ-charm factory, at a $B-$meson factory and a future linear collider. With a relative momentum of the quarks exceeding for instance 3 GeV perturbative QCD should be applicable also in this region. It is, therefore, desirable to push the theoretical prediction as close as possible towards the threshold. The two-loop calculation has been performed more than 40 years ago [25]. The imaginary part of those three-loop diagrams which originate from massless fermion loop insertions in the gluon propagator ("double bubble diagrams") were calculated analytically in [26]. Real and imaginary parts of the purely gluonic correction (and of the double bubble diagrams) were calculated in a semianalytical approach [27] that will be sketched in this subsection.

The polarization function can be written in the form

$$\begin{aligned} \Pi &= \Pi^{(0)} + \frac{\alpha_s}{\pi}\Pi^{(1)} \\ &+ \left(\frac{\alpha_s}{\pi}\right)^2 \left(C_F^2 \Pi_A + C_F C_A \Pi_{NA} + C_F T n_l \Pi_l + C_F T \Pi_F\right) , \end{aligned} \tag{7}$$

where n_l denotes the number of light quark species. Each one of the Π_j is analytical in the complex q^2 plane with a cut from $4m^2$ to $+\infty$. For small

q^2 they can be expanded in a Taylor series

$$\Pi(q^2, m^2) = \sum_{n>0} C_n \left(\frac{q^2}{4m^2} \right)^n . \tag{8}$$

The renormalization condition $\Pi(q^2 = 0, m^2) = 0$ has already been implemented. The evaluation of the Taylor coefficients amounts to the calculation of three loop tadpole integrals with an increasing number of mass insertions — up to 16 for C_8 which is the present limit for the evaluation with the help of algebraic programs.

In the large q^2 region a similar expansion can be performed. For this case the expansion has been performed up to terms of order $(m^2/q^2)^0$ and $(m^2/q^2)^1$. Additional information can be obtained about the behavior close to threshold. Leading and subleading terms can be deduced from the influence of the Coulomb potential in the nonrelativistic region, combined with the knowledge about the logarithmic corrections of the perturbative QCD potential. To extend the range of convergence from $q^2 < 4m^2$ to the full analyticity domain an appropriate variable transformation has to be performed. The data from the three kinematical regions are finally integrated in a Padé approximation which leads to stable results for $\Pi(q^2)$ and $R(s)$ at the same time. The result for the three dominant pieces are shown in Fig. 6 where it is compared to the leading terms close to the threshold and to the high energy approximation.

4.4. Toponium and top quarks in the threshold region

Top quarks were treated as stable particles in the previous section. Although adequate away from the threshold, this approximation is inadequate in the "would-be" toponium region. For a mass of the top quark around 175 GeV a decay rate $\Gamma_t \approx 1.5$ GeV is predicted, corresponding to a toponium width of 3 GeV. The resonances are thus completely dissolved [28, 29], and the individual peaks are merged into a step function like threshold cross section. Quarkonium physics ceases to exist. The large decay rate introduces, however, a cutoff which eliminates all nonperturbative aspects of the interquark potential. Large momentum tails beyond

$$P_{\rm cut} \approx \sqrt{2m_t\Gamma_t} \approx 24 \text{ GeV} \tag{9}$$

or, alternatively, distances above

$$r \approx 0.01 \text{ fm} \tag{10}$$

are irrelevant for the description of the $t\bar{t}$ system [30, 31, 32, 33]. The impact of the large rate is clearly visible in Fig. 7.

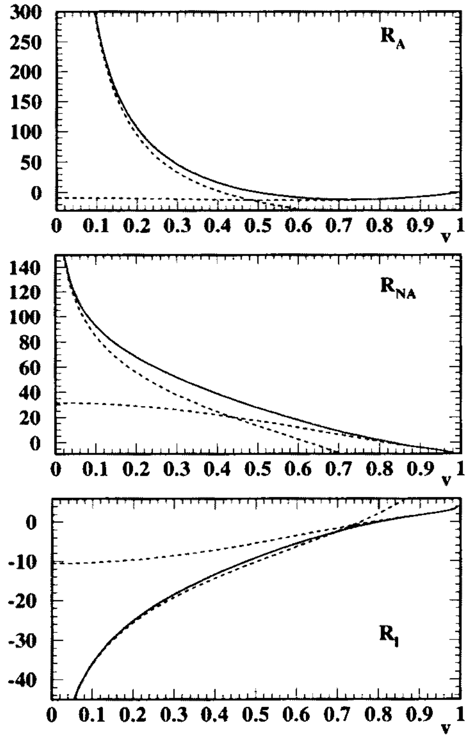

Fig. 6. Complete results plotted against $v = \sqrt{1 - 4m^2/s}$. The high energy approximation includes the m^4/s^2 term.

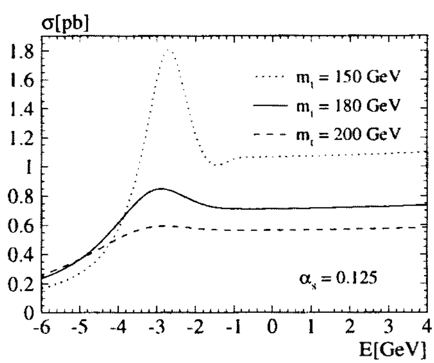

Fig. 7. Total cross section as function of $E = \sqrt{s} - 2m_t$ for three values of the top quark mass.

The predictions for three different top masses $m_t = 150$ GeV, 180 GeV, and 200 GeV corresponding to $\Gamma_t = 0.81$ GeV, 1.57 GeV, and 2.24 GeV demonstrate the strong influence of Γ_t on the shape of the cross section. The shape is furthermore significantly modified by initial state radiation and the spread in the beam energy.

Additional information is encoded in the momentum distribution of top quarks, the "Fermi motion" which can be traced through the decay products $W + b$. This distribution is essentially equivalent to the square of the wave function in momentum space and can, for unstable particles, be evaluated [31, 32, 33] with Green's function techniques (Fig. 8). Various experimental

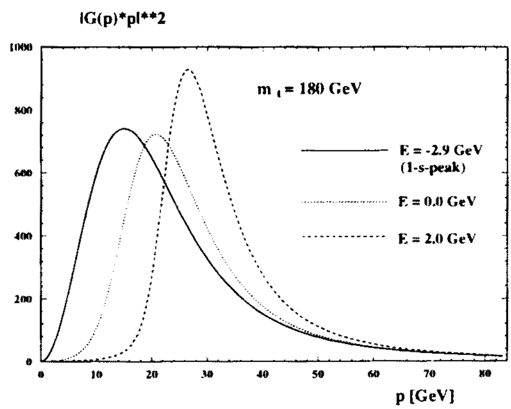

Fig. 8. Momentum distribution of top quarks for three different cms energies.

studies have demonstrated the potential of a linear collider to determine m_t to a precision of perhaps even 200 MeV by measuring the cross section and the momentum distribution simultaneously.

Highly polarized top quarks are required for a variety of precision studies of top decays. In the threshold region this is easily achieved. In fact, even with unpolarized beams top quarks are longitudinally polarized (with a polarization around -0.4) as a consequence of the nonvanishing axial part of the neutral current. Longitudinally polarized beams lead to a fully polarized sample of top quarks.

Another step in complication is achieved by considering the interference between the dominant S and the suppressed P wave contributions. The relative size of these effects is of order $\beta \sim 0.1$. It leads to a forward–backward asymmetry [34] and furthermore to an angular dependent quark polarization perpendicular to the beam direction [35]. A detailed discussion of these effects, in particular of the role of the normal polarization and of rescattering corrections, can be found in [36]. The small polarization of top quarks normal to the production plane is a particularly sensitive measure of the interquark potential.

Additional complications are introduced through the rescattering [36, 37] between b quark jets and the spectator, and by relativistic corrections [32] of order α_s^2. These effects will be important for the quantitative comparison between theory and experiment and the extraction of a precise value for m_t, Γ_t and α_s from threshold studies.

5. Towards NLO in heavy flavor decays

Semileptonic weak decays of bottom mesons and top quarks are particularly clean probes of the fundamental properties of quarks, their masses and mixing angles. Decay rates are, however, influenced by QCD effects, a large part of which can be calculated in PQCD. Leading order corrections to practically all quantities of interest are available: for the decay rate of charmed and bottom quark from [38] and for top quarks from [39]. Lepton decay spectra have been calculated in [40], the energy distribution of hadrons in [41]. Leptons from the decays of polarized quarks exhibit a nontrivial angular distribution [42, 43] and even lepton mass effects have been incorporated in these calculations [44, 45]. A compact summary of most of these QCD corrections can be found in [46].

Different techniques to determine the degree of b or top polarization have been investigated in [43, 47]. The analysis of moments of the lepton momentum distribution, or the ratio of charged vs. neutral lepton moments appear to be particularly promising.

The corrections are often sizable, in particular those to the decay rate. In order to fix the scale in the running coupling constant and to gain confidence in the numerical result, a calculation of NLO corrections to the rate, if not the spectrum, is necessary. Purely fermionic loops have been considered in [48, 49]. In the limit $m_t^2 \gg m_W^2$ the result is particularly simple

$$\Gamma_t = \Gamma_{\text{Born}} \left[1 - \frac{2}{3} \frac{\alpha_{\overline{\text{MS}}}(m_t^2)}{\pi} \left(4\zeta_2 - \frac{5}{2} \right) + \left(\frac{\alpha_{\overline{\text{MS}}}}{\pi} \right)^2 \left(-\frac{2n_f}{3} \right) \left(\frac{4}{9} - \frac{23}{18}\zeta_2 - \zeta_3 \right) \right] \tag{11}$$

with

$$\Gamma_{\text{Born}} = \frac{G_F m_t^3}{8\sqrt{2}\pi} \tag{12}$$

If we adopt the BLM prescription the large coefficient leads to a large shift in the effective scale for α_s: $\mu_{BLM} = 0.12 m_t$. Similarly large correction factors have been observed [50] for the decay of b into $l\nu$ plus a charmed or u quark.

It should be emphasized that the magnitude of NLO corrections $\sim (\alpha_s(m_b^2)/\pi)^2 \approx (0.07)^2$ is well comparable with correction terms obtained in Heavy Quark Effective Theory — typically of order $(\Lambda/m_b)^2 \approx (0.05)^2$. Transitions at zero recoil *i.e.* for the final state with $p_c = \frac{m_c}{m_b} p_b$, are particularly clean from the theoretical point of view. No uncalculable form factor is present, allowing to determine V_{cb} with remarkable precision. The first calculation of the full NLO QCD corrections has therefore been performed at zero recoil [51]. Two important simplifications are present in this case:

- no real radiation has to be considered,
- only relatively simple two loop integrals arise which can be calculated in a series expansion.

The resulting NLO corrections are smaller than the leading ones by about a factor 4, reducing thus the theoretical error by a significant factor. Evidently these results can be considered a first important step towards a complete NLO calculation of the heavy quark decay rate.

REFERENCES

[1] W. Beenakker, H. Kuijf, W. L. van Neerven, J. Smith, *Phys. Rev.* **D40**, 54 (1989). R. Meng, G. A. Schuler, J. Smith, W. L. van Neerven, *Nucl. Phys.* **B339**, 325 (1990). W. Beenakker, W. L. van Neerven, R. Meng, G. A. Schuler, J. Smith, *Nucl. Phys.* **B351**, 507 (1991).

[2] P. Nason, S. Dawson, R.K. Ellis, *Nucl. Phys.* **B303**, 607 (1988); *Nucl. Phys.* **B327**, 49 (1989); *Erratum* **B335**, 260 (1990). G. Altarelli, M. Diemoz, G. Martinelli, P. Nason, *Nucl. Phys.* **B308**, 724 (1988).

[3] F.A. Berends, J.B. Tausk, W.T. Giele, *Phys. Rev.* **D47** (1993) 2746.

[4] E. Laenen, J. Smith, W.L. van Neerven, *Nucl. Phys.* **B369**, 543 (1992); *Phys. Lett.* **B321**, 254 (1994).

[5] E.L. Berger, H. Contopanagos, *Phys. Lett.* **B361**, 115 (1995).

[6] S. Catani, preprint hep-ph/9610413.

[7] S. Catani *et al.*, preprint hep-ph/9602208.

[8] J.H. Kühn, *Theory of Top Quark Production and Decay*, TTP96-18, to be published in the Proceedings of the 1995 SLAC Summer School.

[9] M. Krämer, J. Zunft, P. Zerwas, J. Steegborn, *Phys. Lett.* **B348**, 657 (1995).

[10] G.T. Bodwin, E. Braaten, G.P. Lepage, *Phys. Rev.* **D51**, 1125 (1995).

[11] V. Barger, K. Cheung, W.Y. Keung, *Phys. Rev.* **D41**, 1541 (1990).

[12] K. Cheung, W.Y. Keung, T.C. Yuan, *Phys. Rev. Lett.* **76**, 877 (1996); P. Cho, *Phys. Lett.* **B368**, 171 (1996).

[13] K. Hagiwara *et al.*, *Phys. Lett.* **B267**, 527 (1991); Erratum *Phys. Lett.* **B316**, 631 (1993).

[14] OPAL Collaboration, G. Alexander *et al.*, *Phys. Lett.* **B384**, 343 (1996).

[15] V.M. Driesen, J.H. Kühn, E. Mirkes, *Phys. Rev.* **D49**, 3197 (1994) and refs. therein.

[16] E. Braaten and Yu-Qi Chen, *Phys. Rev. Lett.* **76**, 730 (1996).

[17] H. Fritzsch and J.H. Kühn, *Phys. Lett.* **B90**, 164 (1980).

[18] J.H. Kühn, A. Djouadi, P.M. Zerwas, *Z. Phys.* **C46**, 412 (1990).
K.G. Chetyrkin and J.H. Kühn, *Phys. Lett.* **B248**, 359 (1990).

[19] K.G. Chetyrkin, J.H. Kühn, A. Kwiatkowski, QCD Corrections to the e^+e^- Cross Section and the Z Boson Decay Rate: Concepts and Results, TTP96-06, to be published in *Phys. Rep.*

[20] K.G. Chetyrkin, J.H. Kühn, *Z. Phys.* **C60**, 497 (1993).

[21] K.G. Chetyrkin, O.V. Tarasov, *Phys. Lett.* **B327**, 114 (1994).
S.A. Larin, T. van Ritbergen, J.A.M. Vermasseren, *Phys. Lett.* **B320**, 159 (1994).

[22] K.G. Chetyrkin, J.H. Kühn, *Nucl. Phys.* **B432**, 337 (1994).

[23] K.G. Chetyrkin, J.H. Kühn, *Phys. Lett.* **B342**, 356 (1995).

[24] K.G. Chetyrkin, J.H. Kühn, T. Teubner, Karlsruhe preprint TTP 96-35, hep-ph/9609411.

[25] G. Källen, A. Sabry, *K. Dan. Vidensk. Selsk. Mat.-Fys. Medd.* **29**, No 17 (1955); J. Schwinger, *Particles, Sources, and Fields*, Vol. II, Addison-Wesley, New York 1973.

[26] A.H. Hoang, J.H. Kühn, T. Teubner, *Nucl. Phys.* **B452**, 173 (1995).

[27] K.G. Chetyrkin, J.H. Kühn, M. Steinhauser, *Phys. Lett.* **B371**, 93 (1996), and preprint hep-ph/9606230, in print in *Nucl. Phys.* **B**.

[28] J.H. Kühn, *Act. Phys. Pol.* **B12**, 347 (1981).
J.H. Kühn, *Act. Phys. Austr.* **Suppl.XXIV**, 203 (1982).

[29] I. Bigi, Y.L. Dokshitzer, V.A. Khoze, J. Kühn, P. Zerwas, *Phys. Lett.* **B181**, 157 (1986).

[30] V.S. Fadin, V.A. Khoze, *JETP Lett.* **46**, 525 (1987).
J.M. Strassler, M.E. Peskin, *Phys. Rev.* **D43**, 1500 (1991).

[31] M. Ježabek, J.H. Kühn, T. Teubner, *Z. Phys.* **C56**, 653 (1992).

[32] M. Ježabek, T. Teubner, *Z. Phys.* **C59**, 669 (1993).

[33] Y. Sumino, K. Fujii, K. Hagiwara, H. Murayama, C.-K. Ng, *Phys. Rev.* **D47**, 56 (1993).

[34] H. Murayama, Y. Sumino, *Phys. Rev.* **D47**, 82 (1993).

[35] R. Harlander, M. Ježabek, J.H. Kühn, T. Teubner, *Phys. Lett.* **B346**, 137 (1995).

[36] R. Harlander, M. Ježabek, J.H. Kühn, M. Peter, hep-ph/9604328, Karlsruhe preprint TTP 95-48, in print in Z. Phys. **C**.

[37] K. Fujii, T. Matsui, Y. Sumino, *Phys. Rev.* **D50**, 4341 (1994).

[38] N. Cabibbo, L. Maiani, *Phys. Lett.* **B79**, 109 (1978).

[39] M. Jeżabek, J.H. Kühn, *Nucl. Phys.* **B314**, 1 (1989).

[40] M. Jeżabek, J.H. Kühn, *Nucl. Phys.* **B320**, 20 (1989).

[41] A. Czarnecki, M. Jeżabek, J.H. Kühn, *Acta Phys. Pol.* **B20**, 961 (1989); E: *Acta Phys. Pol.* **B23**, 173 (1992).

[42] A. Czarnecki, M. Jeżabek, J. H. Kühn, *Nucl. Phys.* **B351**, 70 (1991).

[43] A. Czarnecki, M. Jeżabek, J. G. Körner, J. H. Kühn, *Phys. Rev. Lett.* **73**, 384 (1994).

[44] A. Czarnecki, M. Jeżabek, J. H. Kühn, *Phys. Lett.* **B346**, 335 (1995).

[45] M. Jeżabek, L. Motyka, *Acta Phys. Pol.* **B27**, 3603 (1996).

[46] A. Czarnecki, M. Jeżabek, *Nucl. Phys.* **B427**, 3 (1994).

[47] B. Mele, G. Altarelli, *Phys. Lett.* **B299**, 345 (1993).

[48] B. H. Smith, M. B. Voloshin, *Phys. Lett.* **B340**, 176 (1994).

[49] A. Czarnecki, *Acta Phys. Pol.* **B26**, 845 (1995).

[50] M. Luke, M.J. Savage, M.B. Wise, *Phys. Lett.* **B343**, 329 (1995).

[51] A. Czarnecki, *Phys. Rev. Lett.* **76**, 4124 (1996).